Design and Development of Standalone Solar Photovoltaic Battery System with Adaptive Sliding Mode Controller

Surbhi Bagherwal *, Manoj Badoni *, Sunil Semwal**, Shakti Singh* ‡

*Thapar Institute of Engineering and Technology, Patiala India,

**Department of Electrical Engineering, Tula's Institute, Dehradun, India
(loyalsurabchibagherwal@gmail.com, manojbadoni23@gmail.com, sunil.111213@gmail.com)

‡
Corresponding Author; Tel: +91-805-4813-786, shakti.singh@thapar.edu

Abstract- In this paper, a solar photovoltaic-battery located standalone system has been proposed. The configuration of bidirectional buck-boost converter has been proposed for charging (buck) and discharging (boost) the battery storage system. Due to irregular nature of solar radiation and variations in electrical load demand, DC micro grids mostly depend on control methods to overcome with DC link voltage variations and power stability. Adaptive sliding mode controller with washout filter is developed due to its advantages of good strength to an unexpected change of energy resources and loads. This system includes a solar photovoltaic array basis on maximum power tracking from photovoltaic (PV), boost converter to maximize power from the PV array. A bidirectional DC-DC buck-boost converter is developed to charge battery in buck mode and discharge battery in boost mode. Incremental conductance implemented to obtain maximum power from the PV array. The SMC controller performance is verified with different irradiance level (500 and 1000W/m^2) and compared with PI controller performance for the same developed system. For the study resistive load is taken and it is observed that SMC offer reduced overshoot and faster settling time over PI controller under a variety of loading conditions. The simulation model is developed in the MATLAB/Simulink using Sim Power System (SPS) toolbox.

Keywords- Solar photovoltaic, maximum power point tracking, SMC, Washout filter.

Nomenclature

Symbol	Nomenclature	Value	Symbol	Nomenclature	Value
C	DC link capacitance	50μF	I_{sat}	Reverse saturation current	-
L	Inductance	2.5mH	q	Electron charge	1.602 x 10^{-19}
r_L	Inductor resistance	5mΩ	I_{ph}	Photocurrent	-
i_L	Inductor current	-	k	Boltzmann constant	1.38 x 10^{-23}
Q	Battery capacity	150Ah	T	Temperature of the PV	-
V_{int}	Internal battery voltage	-	I_{sso}	Short-circuit current	-
k	Scalar parameter	10	V_{pv}	Photovoltaic voltage	-
ω	Cut-off frequency	283rad/s	k_i	Short circuit current temperature	-
V_{dc}	DC link voltage	380V	T_r	Reference temperature	300K
V_b	Battery voltage	196V	S	Solar irradiation level	-
M	Hysteresis band	0.3796A	I_{rr}	Reverse saturation current at T_r	-
f_{sh}	Switching frequency	10 kHz	E_{gap}	Energy of the band gap for silicon	1.12eV
R_s	Series resistor of PV	-	Ps	Source Power	-
R_p	Parasitic shunt resistor	-	P_L	Load demand	-
I_{pv}	Photovoltaic current	-	R_{eq}	Equivalent resistive load	-

1. Introduction

Now a day, microgrid has been growing to accomplish a superior integration of variable renewable energy source. Moreover, even the districts come to by the national network; a shortage in creating limit has turned out to be basic because of the fast development sought after. Consequently, micro grids will in general abrogate the development of the brought together network [1]. Most without carbon power sources for example, solar photovoltaic and fuel cell, which are immeasurable expanding in number, are additionally DC inherent. These days, almost 30% of all power generated before it is used will go through a power converter device, and it is anticipated to increment to 80% in the next years. The procedure of conversion of energy makes the power loss [2]. It will be increasingly effective and practical if the numbers of conversions are less. Among all the renewable resources, solar power source is the successful contenders because of advantages, such as, accessibility of sun on earth, simplicity of establishment, improve of maintenance, unavailability of moving parts and so on [3]. One of the important disadvantages of solar system is the unpredictable nature of sunlight due to the rotation of the earth and bad climate condition [4]. This course of action gives consistent, continuous and autonomous power supply to the framework load. To neutralize this issue, BESS (battery energy storage system) and MPPT (maximum power point tracking) algorithm has been developed. Incremental conductance (IC) and P&O (Perturb and observe) are two methods which require less calculation and proved to be more accurate [5]. A sliding mode control, fuzzy control is also developed to maximize conversion efficiency of solar PV array [6]. The age from sun oriented photovoltaic cell and capacity through a battery energy-storing framework is least difficult, economical, sensible and exceptionally productive answer for giving access to power in remote and blocked off territories [7]. When the sunlight is not available during night time or in bad weather condition than need of another source arises. The BESS act as a source when sunlight is not available to meet the requirement of power by the load, act as a load while sunlight is in excess, and collect the energy from solar. Therefore, the BESS plays a reliable role when sunlight is not available [8-11]. This system can also be utilized for electric vehicle battery charging in isolated and grid connected enviromet [12-13]. The main objective of this work could be summed up

  ➢ In this paper, an isolated solar PV-battery configuration, with DC-DC boost converter, which additionally connected with the DC load and BESS has been proposed. The MPPT algorithm has been developed to extract maximum power from the solar PV array.
  ➢ Bidirectional DC-DC converter has been designed to interface battery energy storage with the isolated PV system. An adaptive sliding mode controller (SMC) based on washout filter is designed to control switches in the DC-DC bidirectional converter.
  ➢ Performance of proposed SMC controller is compared with the conventional PI controller to present the improved performance of SMC.

This system is developed in MATLAB/SIMULINK environments using a Sim Power System toolbox.

2. System Configuration

The schematic diagram of stand alone solar PV-Battery system is presented in Figure 1. The figure shows that the major component of the system is PV array, battery storage systems and different converters. This system interconnects a limited gathering of DC power sources as solar photovoltaic system, DC power storages as BESS and DC loads that prevalently produce dispense, stores the power, and utilizes this electricity in its local DC loads. The DC-DC boost converter is connected to the solar PV system with maximum power point tracking (MPPT) control algorithm, used to generate gsting pulses for the device used in the converter. The DC-DC bidirectional buck-boost converter is designed to regulate charging and discharging operation of battery used in the system. The control of bidirectional converter is developed using sliding mode control and PI controller. The operation of controllers is discussed in section control algorithm. Designing of the system components is presented in following subsections.

2.1. Design of solar photovoltaic array

Representation of a sunlight based PV cell, consisting of a current source with a diode in parallel as shown in Figure 2. At the output side, series resistor (R_s) and shunt resistor (R_p) are associated. The identical circuit of a sunlight-based photovoltaic cell is displayed below. The design of solar PV panel is modelled by the equation is given below,

$$I_{pv} = n_p I_{ph} - n_p I_{sat} \left[exp\left(\left(\frac{q}{AKT} \right) \left(\frac{V_{pv}}{n_s} + I_{pv} R_s \right) \right) - 1 \right] \qquad (1)$$

Further, I_{ph}, photo current can be calculated as

$$I_{ph} = \left(I_{sso} + k_i (T - T_r) * \frac{S}{1000} \right) \qquad (2)$$

$$I_{sat} = I_{rr} \left(\frac{T}{T_r}\right)^3 exp\left(\left(\frac{qE_{gap}}{kA}\right) * \left(\frac{1}{T_r} - \frac{1}{T}\right)\right) \qquad (3)$$

where, I_{pv} is Photovoltaic current, n_p & n_s is Number of cells in parallel and series, I_{ph} is photocurrent, I_{sat} is reverse saturation current, q is electron charge which is 1.602 x 10-19 C. A is ideality factor, K is Boltzmann constant which is 1.38 x 10-23 J/K, T is temperature of the PV, V_{pv} is photovoltaic voltage, R_s is series resistance of PV cell, I_{sso} is short-circuit current, k_i is short circuit current temperature coefficient, T_r is Reference temperature which is 300 K, S is Solar irradiation level, I_{rr} is Reverse saturation current at T_r, E_{gap} is Energy of the band gap for silicon which is 1.12 eV [14].
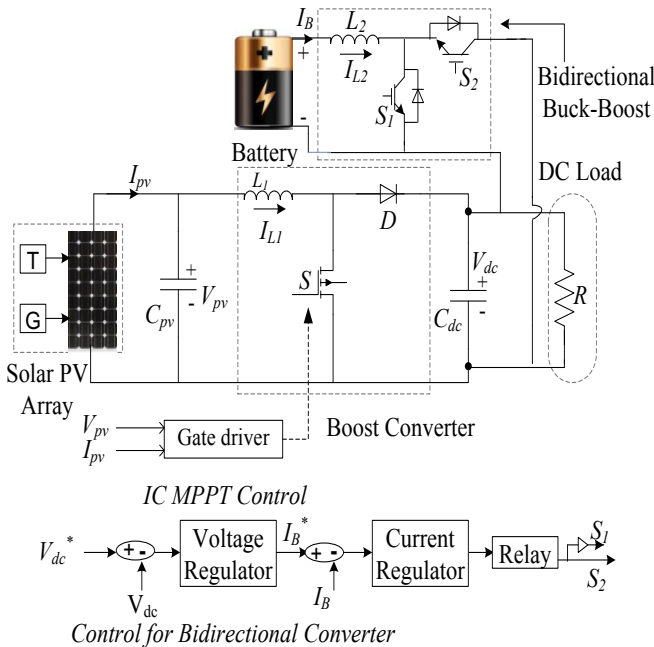
Figure 1. Configuration of standalone solar PV-battery system

The peak power capacity of solar PV array is considered around 1.4kW in this work. As indicated by structure consideration one solar module has V_{oc} of 53.9V and I_{sc} of 3.41A. The general equation of an active power (P) for solar photovoltaic is given below

$$P_{maxM} = V_{mpp} * I_{mpp} \qquad (4)$$

P_{max} = (85% of V_{oc} * 85% of I_{sc}) thus I_{mpp} is 2.89A and V_{mpp} is 45.89V of every module. The measured peak power is give below

$$P_{maxM} = V_{mpp} * I_{mpp} = 1442\ W \qquad (5)$$

It demands peak input voltage of 122.4V and peak input current of 11.78A equivalent to maximum power of 1442 W, to reach up to this voltage (122.4/53.9) and current (11.78/2.89) 3 modules are associated in series and 4 are associated in parallel respectively [15].

2.2 Design of DC-DC boost converter

The DC-DC boost converter is constructed to increase the voltage and the maximum voltage is followed by IC (Incremental conductance) control method which is 122.4V and this voltage is boosted up to 380V [16]. Parameters of the boost converter are as per following
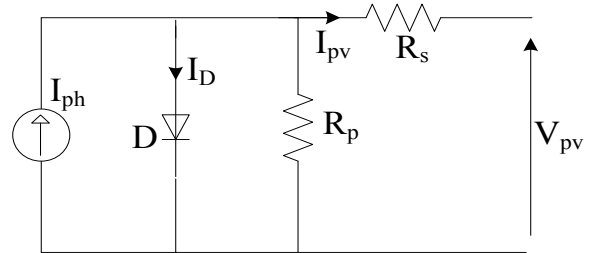

Figure 2. Equivalent circuit of a single photovoltaic cell

$$L_b = \frac{V_{pv}D}{2\Delta i_1 f_{sh}} \qquad (6)$$

$$D = 1 - \frac{V_{in}}{V_b} \qquad (7)$$

where L_b is input inductor, D is duty cycle, $V_{in} = V_{pv}$ is solar PV output voltage, Δi_1 is input current ripple and f_{sh} is the switching frequency. Considering $V_{in} = V_{pv} = 122.4$V to $V_{dc} = 380$V. The measured value of D is 0.678 and for this converter value of f_{sh} is 10KHz and input current ripple is considered as 10% of input current I_1. Therefore, $I_{1 = P/V_{in}} = 11.78$A and $\Delta i_1 = 1.178$A. The value of input inductor L_b is calculated and selected slightly higher value as 5e-5H.

2.3 Modelling of battery

Batteries are an important element in any standalone PV system. As different sorts of batteries are accessible in the market. Most regularly connected in EVs among all are the lithium-ion batteries because of huge energy thickness, long-life stable operation. Equivalent circuit of lithium-ion batteries is displayed in Figure 3. Where R_p and C_p are parasitic resistance and capacitance, V_{int} is internal voltage and R_1 is internal resistance. When the battery is energized the parallel RC network appeared in Figure 3 depicts the transient state of the battery [17]. Subsequently, there will be a few reductions happening over the internal resistance of the battery during this situation. Along these lines, voltage over the battery is not equal as that of internal battery voltage.
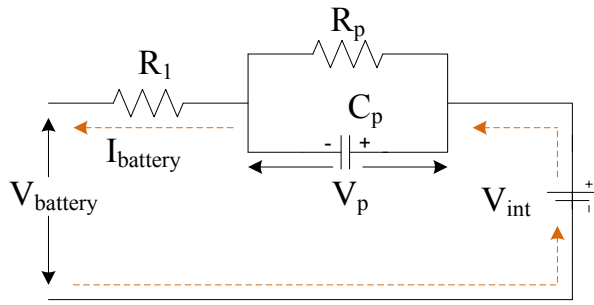
Figure 3. Model of lithium ion battery

Figure 4 shows equivalent circuit of the battery. The charging time taken by the battery can be formulated as by using following steps;

$$V_R = I_{charging} \times R_{SER} \qquad (8)$$

Therefore,

$$V_{battery} = V_R + V_{int} \qquad (9)$$

Hence,

$$V_{battery} = V_{int} + I_{charging} \times R_{SER} \qquad (10)$$

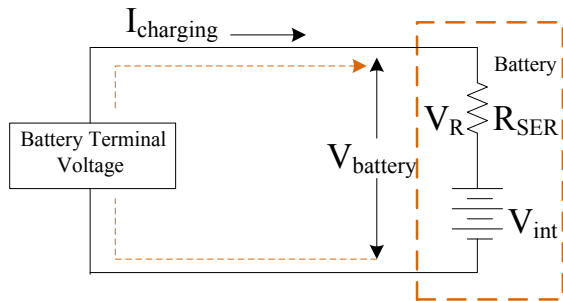Also, cell charge battery voltage is given as,

Figure 4. Equivalent circuit diagram of a battery

$$V_{battery} = \frac{1}{C_{cell}} \int I_{charging}\, dt + V_{int} + I_{charging} \times R_{SER} \quad (11)$$

The maximum cut-off voltage of the lithium-ion battery $V_{batterycutoff}$ can be calculated using Eq. (11) as,

$$\Delta t = \frac{1}{I_{charging}} (V_{batterycutoff} - V_{int} - V \times C) \qquad (12)$$

Hence, Eq. (12) represents the charge time taken by the battery. Here, V_{int} is the initial battery voltage before charging, R_{SER} is the series equivalent resistance of the battery.

3. Control Algorithm

This segment gives information about control methods for various blocks of the proposed system. This section is divided into two parts. In first part, MPPT algorithm is designed to extract maximum power from the solar array and to generate reference voltage. In the second part adaptive sliding mode controller (SMC) is developed to control gating pulses for DC-DC bidirectional converter for the battery energy storage. The detailed design methodology of both the controllers is given below.

3.1. Maximum power point tracking algorithm

The MPPT algorithm is utilized to obtain the extreme power from sun irradiance. It's become necessary to extract all the available power from solar PV arrays. Different MPPT techniques have been used for maximum power extraction in recent literature. The output power from PV arrays is variable not stable due to changes in atmospheric conditions and factors such as solar radiation, temperature and shadow falling on PV arrays. To adjust the extraction power MPPT algorithm becomes a must. MPPT cooperates with DC-DC boost converter to control the duty cycle (D) of the boost converter by following the maximum current and voltage of solar PV system [18]. Incremental conductance (INC) based MPPT algorithm for solar PV system is developed here. The equation for implementing the INC algorithm can be easily derived from the basic power equation. The equation for power is given by using solar PV voltage (V) and current (I) as

$$P = V \times I \qquad (13)$$

Differentiating the above equation with respect to voltage

$$\frac{dP}{dV} = \frac{d\,(V \times I)}{dV} \qquad (14)$$

$$\frac{dP}{dV} = I + V \times \left(\frac{dI}{dV}\right) \qquad (15)$$

The condition for MPPT is that the incline dP/dV should be equal to 0 (zero). Substituting in above equation.

$$\frac{dI}{dV} = -\left(\frac{I}{V}\right) \qquad (16)$$

3.2. Design of SMC controller based on washout filter for DC-DC bidirectional converter

Figure 5 shows solar PV-battery standalone system and Figure 6 shows block diagram of SMC controller. As to obtain the ideal task of battery, a DC-DC buck-boost bidirectional converter is utilized. A SMC based on washout filter is utilized to control I_b. Battery storage converter is planned to keep up power stability of the system and the battery is viewed as a perfect DC voltage source. From Figure 6 we can calculate bus current (i_{bus}) and equivalent resistive load (R_{eq}).

$$i_{bus} = \frac{V_{dc}}{R} + \frac{P_s}{V_{dc}} \qquad (17)$$

$$R_{eq} = \frac{V_{dc}}{i_{bus}} \qquad (18)$$

where V_{dc} is DC bus voltage, i_{bus} is the DC bus current, R is the equivalent resistive load and P_s is the source power.
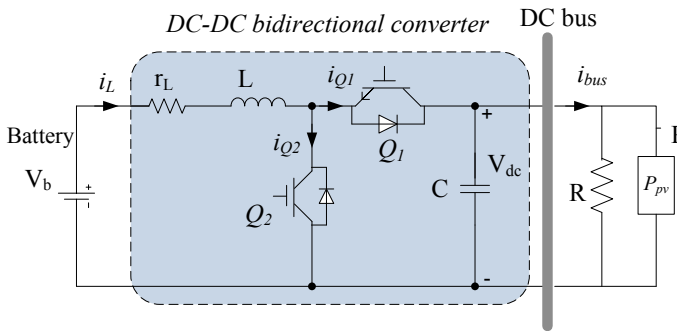

Figure 5. Simplified model of PV-battery model in standalone mode
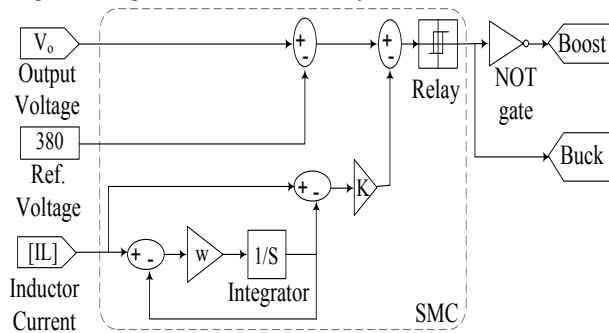

Figure 6. Block diagram of adaptive SMC based on washout filter

This equation can create two situations. In first, when the generated power is greater than or equal to the power demand then load can directly feeds through source power; mean$\{|P_s| \geq |P_L|\}$. In second, when the generated power is less than power demand than a small disturbance can occur in voltage and current; means $\{|P_s| < |P_L|\}$ [19-22]. Therefore, the equivalent load is not linear and because of the varieties in accessible energy source, load can fluctuate over a wide scope of bends. That's why a nonlinear examination is required for a stable operation.

Simplified model of standalone solar-PV-battery model is shown in Figure 5. The dynamics of this model can be represent as,

$$\frac{di_L}{dt} = \frac{1}{L}[V_b - r_L i_L - u V_{dc}] \qquad (19)$$

$$\frac{dV_{dc}}{dt} = \frac{1}{C}\left[u i_L - \frac{V_{dc}}{R} - \frac{P}{V_{dc}}\right] \qquad (20)$$

Where, u is a control input modelled for switches Q1 and Q2, V_b is the input battery voltage, i_L is the inductor current, r_L is the series resistor of the inductor. It is considered that, when Q1 switch is on then Q2 is off and when Q2 is on then Q1 is off. Therefore $u \in \{0,1\}$.

The dynamics can be simplified by scaling the system in amplitude and time.

as $t = \tau \sqrt{LC}$ and $\{i_L, V_{dc}\} = \left\{\sqrt{\frac{C}{L}} V_b x, V_b y\right\}$ respectively.

$$\frac{dx}{d\tau} = 1 - bx - uy \qquad (21)$$

$$\frac{dy}{d\tau} = ux - ay - \frac{d}{y} \qquad (22)$$

Where, $a = \frac{1}{R}\sqrt{\frac{L}{C}}$; $b = \sqrt{\frac{C}{L}} r_L$; $d = \sqrt{\frac{L}{C}}\frac{P}{V_b^2}$, P is the variation between generated power and load demand as $P_{BES} = P = P_S - P_L$.

The Sliding Mode Control based on Washout filter is provided all together to accomplish the following targets; to regulate DC bus voltage, to reduce the transient response during the changing load and to guarantee robustness under changes.

When the standardized inductor current x is gone through a washout filter then we get another signal x_F. Transfer function of x_F is

$$G_F(s) = \frac{X_F(s)}{X(s)} = \frac{s}{s+\omega_n} = \frac{1-\omega_n}{s+\omega_n} \qquad (23)$$

Where, ω_n is the cut off frequency of this filter. In this way, the consideration of the filter include to equation an extra differential condition given by,

$$\frac{dz}{dx} = \omega_n(x - z) \qquad (24)$$

Where, $z = x - x_F$. Representation of the sliding surface, which utilized is as follows.

$$h_n = y - y_r + k_n(x - z) \qquad (25)$$

Where, y_r is the desired DC link voltage, k_n is positive scalar control parameter, z is the lower frequency part of signal x.

$$u = \begin{cases} u^+ = 1, if\ h_n(x) > \mu \\ u^- = 0, if\ h_n(x) < -\mu \end{cases} \qquad (26)$$

Where, μ is constant, which limits the hysteresis band

$$\mu = \frac{V_b(V_{dc}-V_b)}{2Lf_sV_{dc}} \qquad (27)$$

Now it's important to renormalize the factors of the system.

$$\omega = \frac{\omega_n}{\sqrt{LC}} \ , k = k_n\sqrt{\frac{L}{C}}$$

Where, C is the DC link capacitor, L is the inductance of DC-DC bidirectional converter, f_s is the switching frequency,

247

μ is the hysteresis band, ω is cut-off frequency, k is scalar parameter and Q is the battery capacity. After all the parameters have been resolved, the estimations of those parameters are at that point connected in the control block. The values of calculated parameters are given in the Appendix.

4. Results and Discussion

The proposed solar-PV-battery system and SMC controller with washout filter is developed using MATLAB/SIMULINK. The results of the standalone solar PV-battery power producing system are explained in this segment. It includes performance of the system with variation in solar irradiance, DC link voltage regulation and variation in load. Comparative performance of proposed SMC with a conventional PI controller is also presented. A detailed discussion is presented as follows.

4.1 Performance of the system with variation in solar irradiance

The current-voltage (I-V) and power-voltage (P-V) curves of PV module at 500 W/m² & 1000 W/m² are depicted in Figure 7. It is demonstrated in the figure that the generated power from the solar photovoltaic array has varied with time. İt is observed from these waveforms that the maximum power generated by the PV array at 1000W/m² is 1.5kW, whereas at 500 W/m² power is 7.5kW. Various irradiance levels for solar photovoltaic arrays are formed. The results of the voltage of DC bus shown in Figure 8. Battery energy storage can mark the bus voltage with the variation in solar photovoltaic array. Inductor current during variation in solar irradiance is shown in Figure 9. In PI control, moreover induces the comparative outcome with the SMC, main distinctive is PI control incites additional swaying contrasted with the SMC when the transients occur. In Figures 8 & 9 SMC drawn with red line and PI drawn with dashed blue line. Figure 10 shows the power balance in standalone mode. Solar power, battery power and load power drawn with red, blue and green respectively. The total time of simulation run is 0.35s.

4.2 Regulation of voltage at DC link with SMC and PI

In this case, the load is taken as 160Ω and run it up to 0.05sec. These results shows there is no overshoot in SMC when compared with PI controller performance and also SMC is faster settling time than PI. Figure 11 shows DC link capacitor output voltage, it is observed from this result that initially PI controller shows overshoot 395V and SMC controller gives less overshoot around 380V. Inductor current results during DC link voltage regulation is shown in Figure 12. PI has been drawn with dashed blue line and SMC has been drawn with a red line. It is observed from this result that inductor current achieves its steady state value faster with SMC controller.
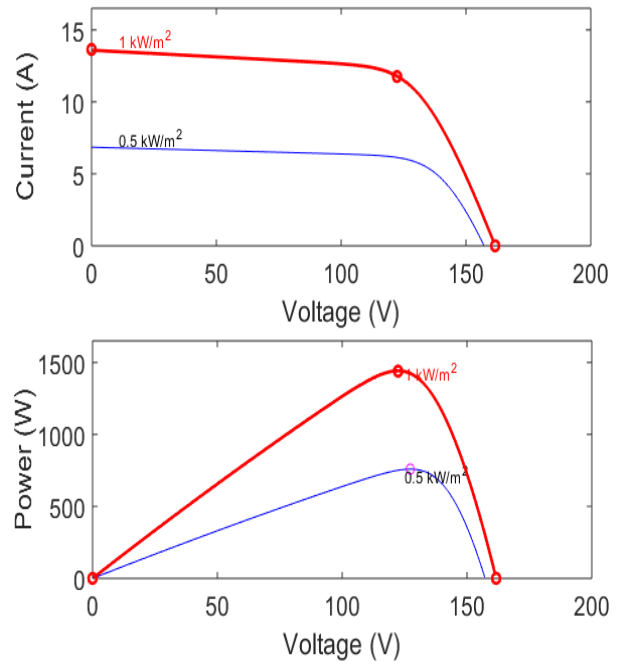

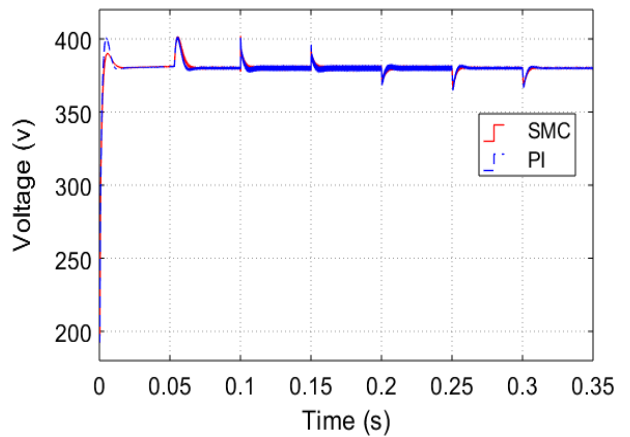Figure 7. P-V and I-V characteristics of solar photovoltaic array

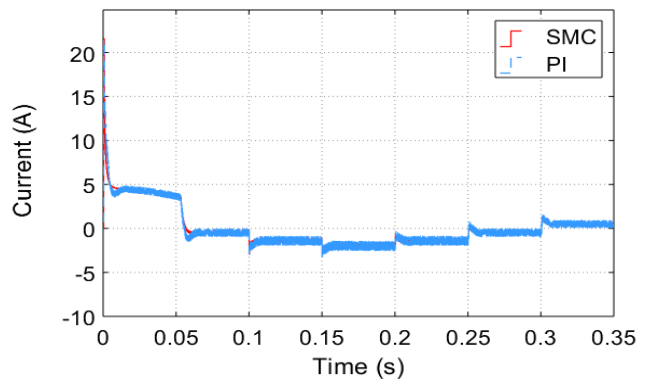Figure 8. Output voltage of DC link capacitor

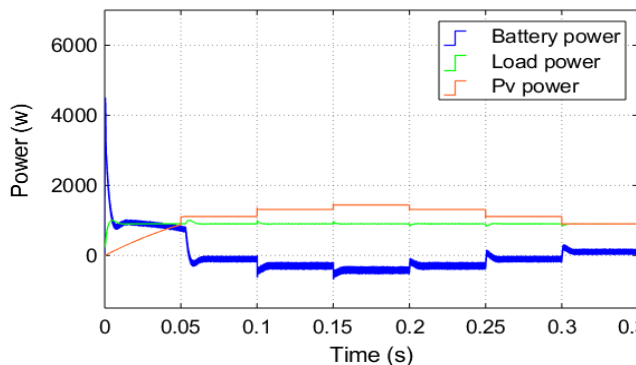Figure 9. Inductor current during solar irradiance variation

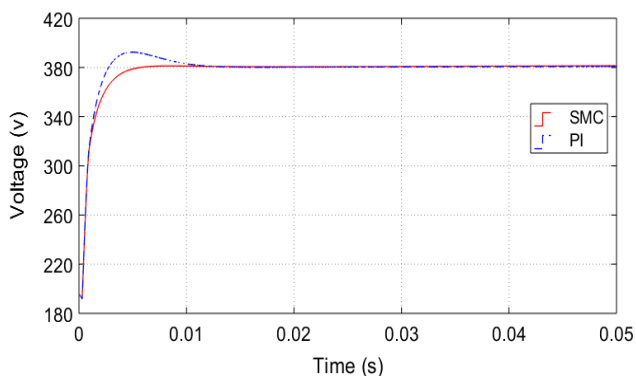Figure 10. Power balance in standalone solar PV system
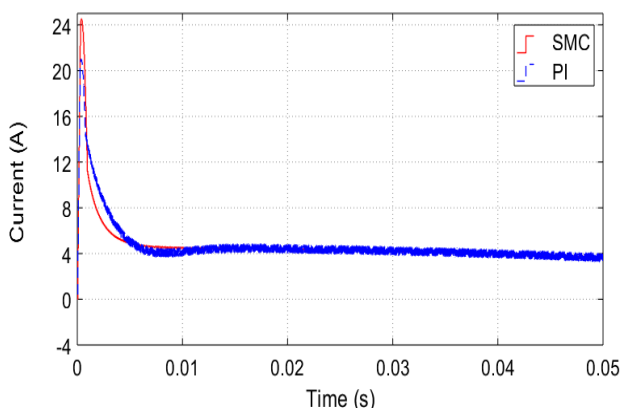

Figure 11. Output voltage of DC link capacitor

Figure 12. Inductor current results during variation in voltage regulation

4.3 Performance of the system with variation in load

The results of load variation are examined in this section. In this case, the load resistances value is varied as 350Ω, 250Ω, 150Ω, 250Ω and 350Ω respectively, with the time duration of 0.1s and the total simulation time is 0.5s. Figure 13 shows variation in DC link voltage with load changing. It is observed from this result that upon changing value of load in different steps, the DC link voltage value settle faster with SMC than the PI controller. As shown in result with initial load variation DC link voltage overshoot up to 400V with PI, whereas it overshoot upto 385V with SMC. Figure 14 shows the inductor current result with variation in load, it is observed that inductor current achieves steady state value fast with SMC than PI controller. It can be seen that, when the resistance load is minimized then the voltage dip is

occurring in the result and when resistance load is maximized then voltage swell is occurring. When the overshoot voltage and undershoot voltage is occuring SMC has Improved results than the PI control.
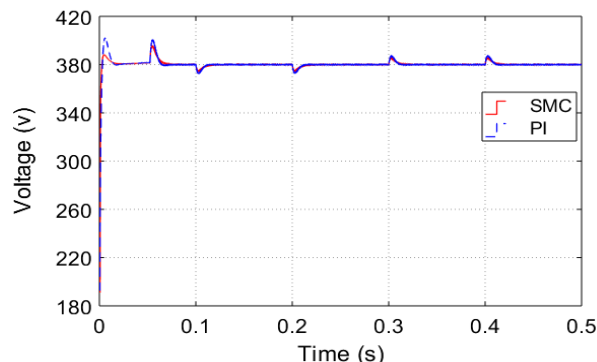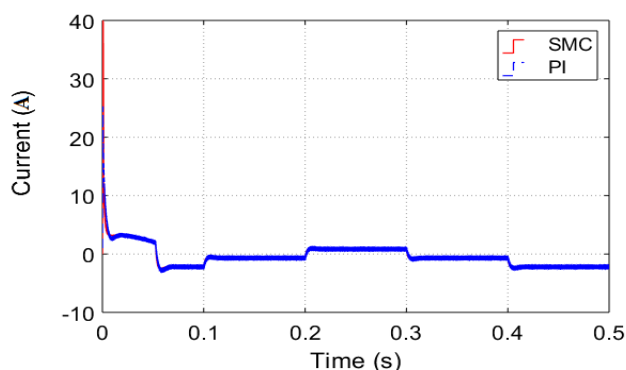

Figure 13. Output voltage of DC link capacitor

Figure 14. Inductor current during variation in load

5.   Conclusion

To keep the stable operation of bidirectional DC-DC buck-boost converter in standalone solar PV-Battery system with DC loads, an SMC with Washout Filter has been proposed. For the execution of SMC, a MATLAB/ SIMULINK model has been directed. Through the control of bidirectional DC-DC buck boost converter for the battery charging and discharging process, SMC method with Washout Filter has been found to keep the stable operation of the DC bus and maintain the power balance of the system. An SMC controller gives a superior performance on the transients in cases of variable solar irradiation or the consumption of the loads is changing, compared to the conventional PI controller method. The overshoot in case of PI controller is observed around 395V and 400V in steady loading and variable loading condition, whereas it is observed 380V and 385V in case of SMC controller respectively. Moreover, this current through the inductor achieve steady state value fast with an SMC controller than the PI controller used in the similar system. An SMC provides better results in comparison with PI Control on voltage overshoot and voltage undershoots. The overall performance of the standalone solar PV-battery

system with SMC controller has been found satisfactory as indicated in the results.

References

[1] Md A. Hossain, H. R. Pota, Md J. Hossain and F. Blaabjerg, "Evolution of microgrids with converter-interfaced generations: Challenges and opportunities", International Journal of Electrical Power & Energy Systems, Vol.109 (2019) pp 160-186. (Article)

[2] B. K. Boss, Global warming: Energy, environmental pollution, and the impact of power electronics, IEEE Ind. Electron. Mag. 4 (2010) pp 6-17. (Book Article)

[3] M. Badoni, A. Singh, V. P. Singh and R. N. Tripathi, "Grid interfaced solar photovoltaic system using ZA-LMS based control algorithm", Electric Power Systems Research, Vol. 160 (2018) pp 261-272. (Article)

[4] S. Senguttuvan and M. Vijayakumar, "Solar Photovoltaic System Interfaced Shunt Active Power Filter for Enhancement of Power Quality in Three-Phase Distribution System", Journal of Circuits Systems and Computers, Vol. 27 (2016) 1850166. (Article)

[5] A. K. Podder, N. K. Roy and H. R. Pota, "MPPT methods for solar PV systems: a critical review based on tracking nature", IET Renewable Power Generation, Vol. 13 (2019) pp 1615-1632. (Article)

[6] M. K. Al-Nussairi, R. Bayindir and E. Hossain, "Fuzzy logic controller for DC-DC buck converter with constant power load", Proc. IEEE 6th International Conference on Renewable Energy Research and Applications (ICRERA), (San Diego, CA, 2017) pp. 1175-1179. (Conference Paper)

[7] N. Saxena, I. Hussain, "Implementation of a grid-integrated PV-battery system for residential and electrical vehicle application", IEEE Transaction on Industrial Electronics, Vol. 65 (2018) pp 6592 - 6601. (Article)

[8] H. Kim, B. Parkhideh, T. D. Bongers and H. Gao, "Reconfigurable solar converter: A single-stage power conversion PV-battery system", IEEE Transactions on Power Electronics, Vol. 28 (2013) pp 3788-3797. (Article)

[9] A.S. Sener, "Improving the life-cycle and SOC of the battery of a modular electric vehicle using ultra-capacitor", Proc. 8th International Conference on Renewable Energy Research and Applications (ICRERA), (Brasov, Romania, 2019) pp. 611-614. (Conference Paper)

[10] A. Fleischhacker, H. Auer, G. Lettner and A. Botterud, "Sharing solar PV and energy storage in apartment buildings: resource allocation and pricing", IEEE Transactions on Smart Grid, Vol .10 (2019) pp 3963-3973. (Article)

[11] E. Irmak and N. Güler, "Application of a boost based multi-input single-output DC/DC converter", Proc. IEEE 6th International Conference on Renewable Energy Research and Applications (ICRERA), (San Diego, CA, 2017) pp. 955-961. (Conference Paper)

[12] I. Cetinbas, B. Tamyürek and M. Demirtas, "Energy management of a PV energy system and a plugged-in electric vehicle based micro-grid designed for residential applications", Proc. 8th International Conference on Renewable Energy Research and Applications (ICRERA), (Brasov, Romania, 2019) pp. 991-996. (Conference Paper)

[13] A. Belkaid, I. Colak, K. Kayisli and R. Bayindir, "Design and implementation of a Cuk converter controlled by a direct duty cycle INC-MPPT in PV battery system", International Journal of Smart Grid, Vol. 3(2019) pp 19-25. (Article)

[14] H. Beltran, E. Perez, and N. Aparicio, "Daily solar energy estimation for minimizing energy storage requirements in PV power plants", IEEE Transactions on Sustainable Energy, Vol. 4 (2013) pp 1949-3029. (Article)

[15] C. Jain and B. Singh, "A three-phase grid tied SPV system with adaptive DC link voltage for CPI voltage variations", IEEE Transaction on Sustainable Energy, Vol. 7 (2016) pp 337-344. (Article)

[16] R. J. Wai and S. J. Jhung, "Design of energy-saving adaptive fast-charging control strategy for li-fe-po4 battery module", IET Power Electronics, Vol. 5 (2012) pp 1684–1693. (Article)

[17] K. Kumar, N. R. Babu and K. R. Prabhu, "Design and analysis of an integrated Cuk-SEPIC converter with MPPT for standalone wind/PV hybrid system", International Journal of Renewable Energy Research, Vol. 7 (2017), pp 96-106. (Article)

[18] K. Ishaque, Z. Salam and G. Lauss, "The performance of perturb and observe and incremental conductance maximum power point tracking method under dynamic weather conditions", Applied Energy, Vol. 19 (2014) pp 228-236. (Article)

[19] S. Singh, D. Fulwani and V. Kumar, "Robust sliding-mode control of DC-DC boost converter feeding a constant power load", IET Power Electronics, Vol. 8 (2015) pp 1230-1237. (Article)

[20] E. Ponce and D. Pagano, "Sliding dynamics bifurcations in the control of boost converters", Proc. IFAC World Congress, 2011 (Milan, September 2011), pp. 1–6. (Conference Paper)

[21] L. Saihi, Y. Bakou, A. Harrouz, I. Colak, K. Kayisli and R. Bayindir, "A Comparative study between robust control sliding mode and backstepping of a DFIG integrated to wind power system", Proc. 7th International Conference on Smart Grid (icSmartGrid), (Newcastle, Australia, 2019) pp. 137-143. (Conference Paper)

[22] S. Singh, D. Fulwani and V. Kumar, "Robust sliding-mode control of DC-DC boost converter feeding a constant power load", IET PowerElectronics, Vol. 8 (2015) pp 1230-1237. (Article)